IIF-SAS Report

Load Forecasting for Special Days Using a Rule-based Modeling Framework: A Case Study for France

Siddharth Arora[†] and James W. Taylor[*]

Saïd Business School,
University of Oxford, Park End Street, Oxford, OX1 1HP, U.K.

† Siddharth.Arora@sbs.ox.ac.uk

* James.Taylor@sbs.ox.ac.uk

Load Forecasting for Special Days Using a Rule-based Modeling Framework: A Case Study for France

Abstract

This paper presents a case study on short-term load forecasting for France, with emphasis on special days, such as public and national holidays. Existing methods for load forecasting focus mainly on normal working days, while special days are often ignored during the modeling process. We generate short-term load forecasts for normal and special days in a coherent and unified framework, using a rule-based methodology. The proposed methodology encapsulates prior domain knowledge of load profiles into the statistical model. In addition to special day effects, we accommodate the intraday, intraweek, and intrayear seasonality in load, whereby we consider the original version and corresponding rule-based triple seasonal adaptation of Holt-Winters-Taylor (HWT) exponential smoothing, seasonal autoregressive moving average (SARMA), artificial neural networks (ANNs), along with intraday and intraweek singular value decomposition (SVD) based exponential smoothing methods. Using nine years of half-hourly load for France, we evaluate point and density forecasts, for lead times ranging from one half-hour up to a day ahead. Overall, the rule-based SARMA method generated the most accurate point and density forecasts.

Keywords: Point and density forecasts; Rule-based; Short-term; Special days; Triple seasonal.

1. Introduction

Accurate short-term forecasts of electricity demand (*load*) are crucial for making informed decisions regarding unit commitment, energy transfer scheduling, and load-frequency control of the power system. An electric utility needs to make these operational decisions on a daily basis, often in real-time, in order to operate in a safe and efficient manner, optimize the operational costs, and improve the reliability of distributional networks. Moreover, inaccurate forecasts can have substantial financial implications for energy markets (Charytoniuk and Chen 2000).

Given the significance of short-term load forecasts for electric utilities and energy markets, a plethora of different modeling approaches have been proposed for forecasting load for normal days (Bunn 2000). Modeling load for special days, such as public holidays and long weekends, however, has usually been overlooked in the research literature (see, for example, Smith 2000; Nowicka-Zagrajek and Weron 2002; Hippert *et al.* 2005; Taylor 2010a). We refer to load observed on normal days as *normal load*, whereas load observed on special days is referred to as *anomalous load*.

The lack of attention in modeling anomalous load can be attributed to the following reasons: 1) Anomalous load deviates significantly from normal load, which necessitates special days to be treated as being different from normal days. 2) The relative infrequent occurrence of special days (special days tend to occur annually) results in the unavailability of an adequate number of anomalous observations required for sufficiently training the model. 3) Different special days exhibit different *load profiles* (shape of the intraday load curve), which requires each special day to be modeled as having a unique profile. The aforementioned reasons make statistical modeling of anomalous load very challenging, due to which, the task of forecasting anomalous load has often been left to the expert judgment and decision of the central controller of the electricity grid

(Hyde and Hodenett 1993; 1997). The focus of this study is to develop models that can potentially be deployed in a real-time automated online system, which can assist the central controller make informed decisions under normal and anomalous load conditions.

Although special day effects are often ignored during the modeling, the choice of replacing or smoothing anomalous load is subjective and not well-defined. Smith (2000) treats special days as a recent Sunday during the modeling process. Nowicka-Zagrajek and Weron (2002) employ anomalous load observations for model estimation, but ignore special day effects during model evaluation. Hippert *et al.* (2005) avoid special days by replacing them in their modeling, by load observed on a corresponding normal day of the week from the last week. Prior to estimation and evaluation procedures, Taylor (2010a) smoothes out the load for special days, by replacing it with the mean estimate of the normal load from the corresponding periods of the two adjacent weeks. Crucially, the problem with ignoring anomalous load is that it not only guarantees that the resulting model cannot be used for special days, but it also results in considerably large forecast errors on normal days that lie in the vicinity of special days. In this study, we use the actual load time series for modeling, whereby the anomalous load observations are neither replaced, nor smoothed out.

Multivariate weather-based models have been employed previously for modeling load (Cottet and Smith 2003; Dordonnat *et al.* 2008). Multivariate models utilize weather variables like temperature, wind speed, cloud cover, and humidity, along with the historical load observations. Univariate models on the other hand, include only the historical load observations, and have been shown to be adequate for short-term load forecasting (Taylor 2008). It has been argued that the weather variables tend to vary smoothly over short time scales, and this variation can be captured in the load data itself (Bunn 2000). Moreover, for short lead times, univariate models have been

shown to be competitive with weather-based models (Taylor 2008). Hence, we employ univariate methods for short-term load forecasting in this study.

Rule-based forecasting has received considerable attention in the forecasting research community (see, for example, Armstrong 2001; 2006). The rationale of using a rule-based approach lies in incorporating subjective judgment based on domain knowledge and expertise into the statistical model. It has been argued that rule-based forecasting can outperform conventional extrapolation methods, especially in cases where prior domain knowledge is available and the time series exhibits a consistent structure (see, for example, Bunn and Wright 1991; Collopy and Armstrong 1992; Adyaa *et al.* 2000). A discussion on the issues of using a rule-based approach with statistical forecasting methods is provided by Bunn and Wright (1991). Collopy and Armstrong (1992) create a rule-base to combine forecasts from different extrapolation methods, and report that rule-based methods reduced the forecast error by approximately half compared to an equally-weighted combined forecast. Adyaa *et al.* (2000) emphasize that the identification of relevant features or characteristics of a time series is crucial for the success of rule-based methods. Given that the task of forecasting anomalous load has previously relied mainly on subjective judgment, and the fact that load exhibits a consistent prominent structure (triple seasonality), we adopt a rule-based methodology in this study. We incorporate domain knowledge into the statistical models via rules. The rationale of the proposed rule lies in identifying the most suitable historical special day, whose anomalous load observations would be most useful in improving the accuracy of the model in forecasting load for the future special day.

In a recent study, Arora and Taylor (2013) propose a rule-based approach for modeling anomalous load for Great Britain (GB). This paper extends the work of Arora and Taylor (2013),

whereby we: 1) Adapt the rules and models proposed earlier for GB, in order to model load for France. 2) Propose a new method; referred to as the rule-based intraday SVD based exponential smoothing method. 3) Evaluate density forecasts (in addition to point forecasts), across normal and special days. To the best our knowledge, there are no existing studies on modeling the density of anomalous load. Moreover, compared to GB, we note that modeling anomalous load for France is more challenging, due to the relatively large number of different types of special days observed in France.

Although we demonstrate the applicability of the rule-based methods for load forecasting, the proposed methodology can potentially be adapted for other applications. Some examples where this approach could be useful for forecasting includes call centre arrivals, hospital admissions, cash withdrawals at ATMs, water usage, and transportation counts, as the corresponding time series exhibit seasonality and anomalous conditions pose significant modeling challenges.

In the next section, we provide a comprehensive review of the literature on modeling anomalous load. We present the French load data in Section 3, and discuss the normal and anomalous load characteristics. In Section 4, we present the rule-based methods. Section 5 presents the subjective formulation of a rule. Empirical comparison of different methods and simple benchmarks is provided in Section 6. In Section 7, we summarize and conclude the paper.

2. Review of Methods for Anomalous Load Forecasting

Previous approaches for short-term forecasting of normal and anomalous load have mostly employed regression-based methods with dummy variables for special days (see Ramanathan *et al.* 1997; Pardo *et al.* 2002; Cottet and Smith 2003; Cancelo *et al.* 2008; Soares and Medeiros 2008; Dordonnat *et al.* 2008; De Livera *et al.* 2011; Kim 2013).

Ramanathan *et al.* (1997) build a separate regression model for each hour of the day, and include special day and weather effects on load using dummy variables. Pardo *et al.* (2002) use dummy variables for capturing the day of week, month of year, and holiday effects on load. Moreover, following the work of Ramanathan *et al.* (1997), Pardo *et al.* (2002) employ additional dummy variables for the day following a special day. This helps accommodate the potential impact of anomalous load on a normal day following a special day. Cottet and Smith (2003) model load using a multi-equation Bayesian model. They treat Christmas Day, Boxing Day, New Year's Day, Good Friday, and Easter Monday as the most idiosyncratic public holidays, and allot a different dummy variable to each of the above mentioned public holidays, while all other remaining holidays in the dataset were allotted a single dummy variable. Moreover, Cottet and Smith (2003) use 48 coefficients for each dummy variable to capture the intraday seasonality using half-hourly load. Cancelo *et al.* (2008) build a separate model for each hour of the day using Spanish load. They first issue a forecast for load assuming a normal day, and make adjustments accordingly for special days using different dummy variables employed for different classes of special days. Soares and Medeiros (2008) build a two stage model for each hour of the day for load, such that anomalous load is modeled in the first stage using dummy variables. Any unexplained component in load is then modeled in the second stage using either an autoregressive (AR) model or an ANN. However, Soares and Medeiros (2008) found that using an ANN did not lead to any improvement in forecast accuracy over a linear AR model. Dordonnat *et al.* (2008) build a regression model for each hour of the day, and accommodate special day effects using dummy variables. In addition, they also use dummy variables for *bridging days*. A day is defined to be a bridging day if it is a Monday before a special day, or a Friday after a special day. The load on bridging days tends to be lower than normal load, and

hence, needs to be treated separately. De Livera *et al.* (2011) propose an innovations state space modeling framework, and handle special day effects for national and religious holidays in load via dummy variables. Kim (2013) adopt a double seasonal multiplicative SARMA model to accommodate special day effects on an hourly basis using dummy variables for Korean load.

To model load adequately, the triple seasonal effects need to be accommodated, which requires different dummy variables for identifying the period of the day, day of the week, and date, for each special day. Given that load for different special days is different, dummy variables are also required for identifying the special day type. However, to include a correction coefficient with each dummy variable results in the final model being highly parameterized and difficult to interpret. To avoid the model becoming over-parameterized, different special days have often been classified as belonging to the same special day type (see, for example, Kim *et al*. 2000; Cottet and Smith 2003; Cancelo *et al.* 2008; Soares and Medeiros, 2008; Dordonnat *et al*. 2008). The classification of special days relies on the assumption that load profile for different special days can be treated as being similar, and would remain similar over the years. Using French load, we observe from the data that each special day exhibits a unique profile. Hence, instead of classifying different special days as being the same, we model each special day as having a unique profile, which may change over different years.

Apart from regression-based methods, some authors have proposed rule-based approaches for anomalous load forecasting (Rahman and Bhatnagar 1988; Hyde and Hodnett 1997; Arora and Taylor 2013), while others have used ANNs (Srinivasan *et al*. 1995; Kim *et al*. 2000, Song *et al*. 2000). Rahman and Bhatnagar (1988) propose a rule-based approach, whereby they formulate rules based on the logical and syntactical relationships between weather and load, using data for an electric utility in Virginia, USA. Hyde and Hodnett (1997) formulate rules for

the Irish load data, whereby the rationale of their approach is to find the deviation of load for different special days from normal load for a given year, and use this deviation as a correction term for the corresponding special day falling next year. Srinivasan *et al*. (1995) use ANNs with fuzzy rules, and find that the load profile on most special days is similar to the profile of a typical Sunday. Kim *et al*. (2000) classify special days into five different types, and employ an ANN (for each special day type) used in conjunction with fuzzy rules inferred from the Korean load data. Song *et al*. (2000) propose a fuzzy linear regression method, and report that errors from their method were lower compared to an ANN and fuzzy inference method. Apart from fuzzy rules, ANNs have also been used in conjunction with self-organizing maps (SOMs) for anomalous load forecasting (Lamedica *et al.* 1996).

It is noteworthy that most existing methods for anomalous load forecasting rely on classifying different special days as being the same, while some approaches employ different models for normal and special days (Kim *et al*. 2000). We, however, treat each special day as having a unique profile, and adopt a unified modeling framework for both day types. Moreover, the existing rule-based methods are tailored only to the data at hand (Rahman and Bhatnagar 1988; Hyde and Hodnett 1993; 1997). This makes the task of adapting existing rule-based methods to different datasets very challenging, as it would require creating a completely new set of rules for the French data. Due to the aforementioned reasons, we do not use existing rule-based methods as benchmarks in this study.

3. Anomalous Load Characteristics

We employ nine years of half-hourly load for France, stretching from 1 January 2001 to 31 December 2009, inclusive. This leads to a total of 157,776 load observations. We use the first eight years of the dataset as the estimation sample (consisting of 140,256 observations), and

employ the final year as the evaluation sample (consisting of 17,520 observations). We generate forecasts by rolling the forecast origin through each period in the post-sample data. The data has been obtained from Électricité de France (EDF), and there are no missing observations in the employed dataset.

The complete load data is presented in Figure 1. It can be seen from this figure that load exhibits a recurring within-year pattern (due to seasonal effects), termed as the intrayear seasonality. Moreover, the data shows an upward trend. Also, load in winter is higher than in summer, which is due to the increased use of electrical equipment for heating in winter in France.

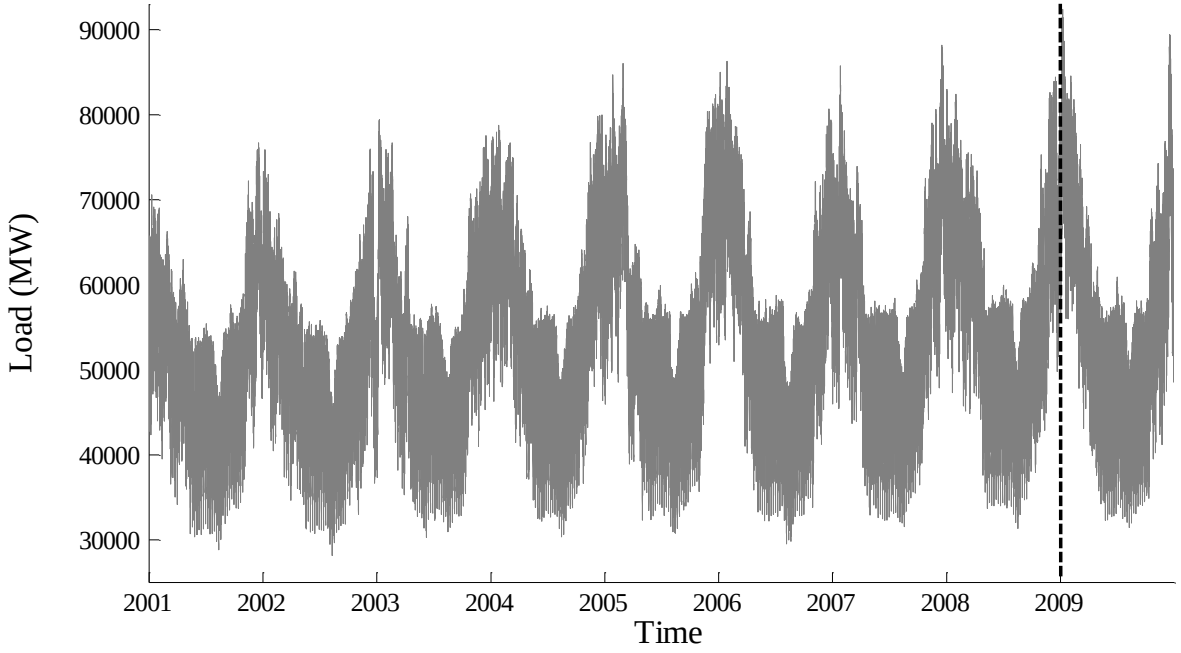

Figure 1— Half-hourly load for France stretching from 1 January 2001 to 31 December 2009. The vertical dashed line denotes the time index that divides the time series into non-overlapping estimation and evaluation sample.

The average intraday cycle (calculated using only the estimation sample) for different days of the week is presented in Figure 2. It can be seen from the figure that load on weekends is considerably lower compared to weekdays, whereby load is lowest on Sundays. Load on

Monday mornings and Friday evenings is particularly lower compared to other weekdays (for the same period of the day), whereas the average load profiles for Tuesday, Wednesday and Thursday are very similar.

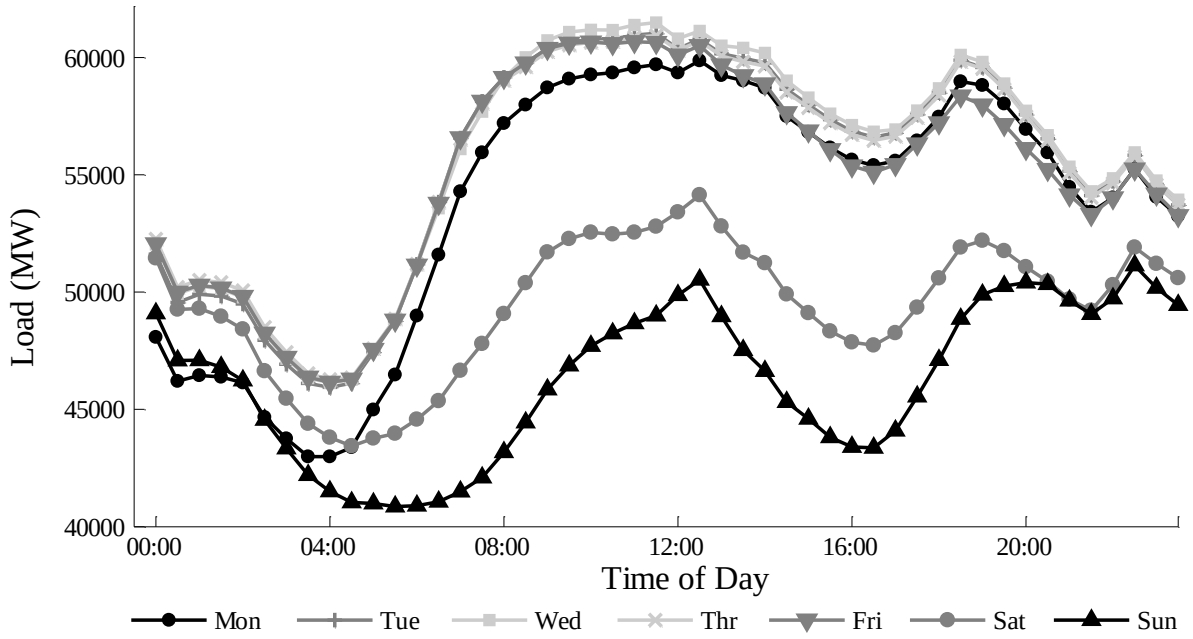

Figure 2— Average intraday profile for each day of the week.

Using the calendar dates for French public holidays, we identified a total of twenty four special days in the one year post-sample data. Inspection of the data reveals that load for a given special day is considerably lower than normal day, for the same day of the week, around the same date. It is noteworthy that some authors have employed objective schemes for identifying special days (Lamedica *et al*. 1996). To compare anomalous and normal load, in Figure 3, we plot load for a Bastille Day (14 July 2008, Monday), which is a national holiday in France, and load for a normal working Monday from the preceding and following weeks. It is evident from Figure 3 that not only anomalous load is substantially lower than normal load, but the load profiles for normal and special days are indeed very different. Inspection of the data reveals that this characteristic of anomalous load holds true across all special days.

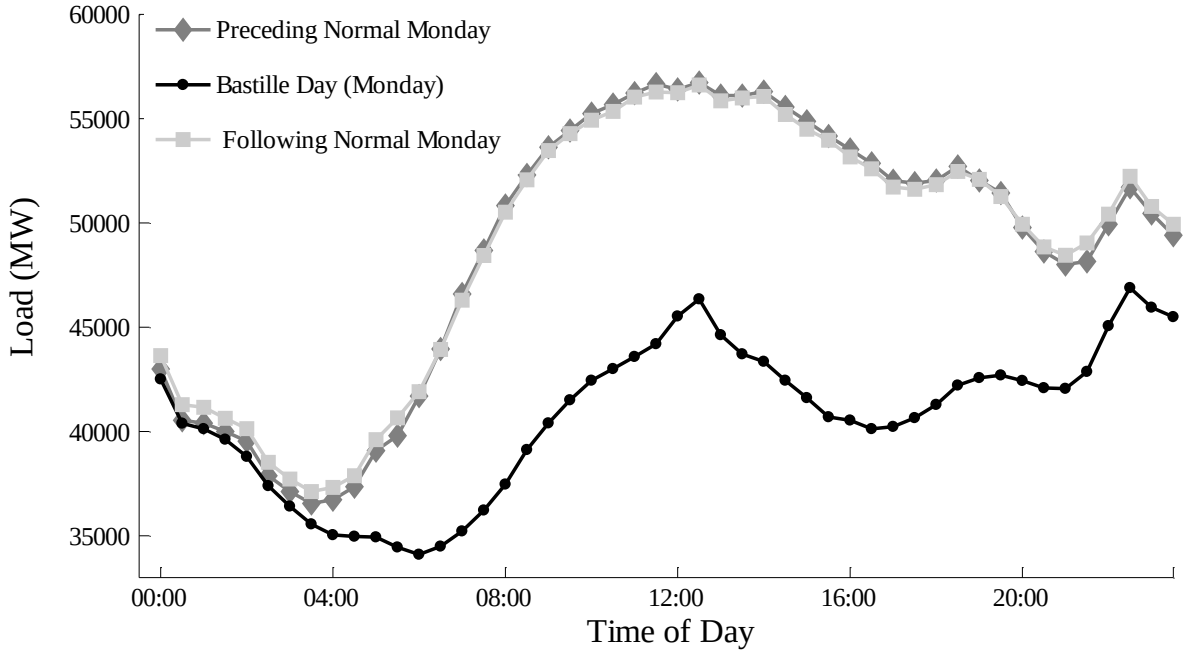

Figure 3— Load profile for a Bastille Day (14 July 2008, Monday), a normal Monday (7 July 2008) from the preceding week, and a normal Monday (21 July 2008) from the following week.

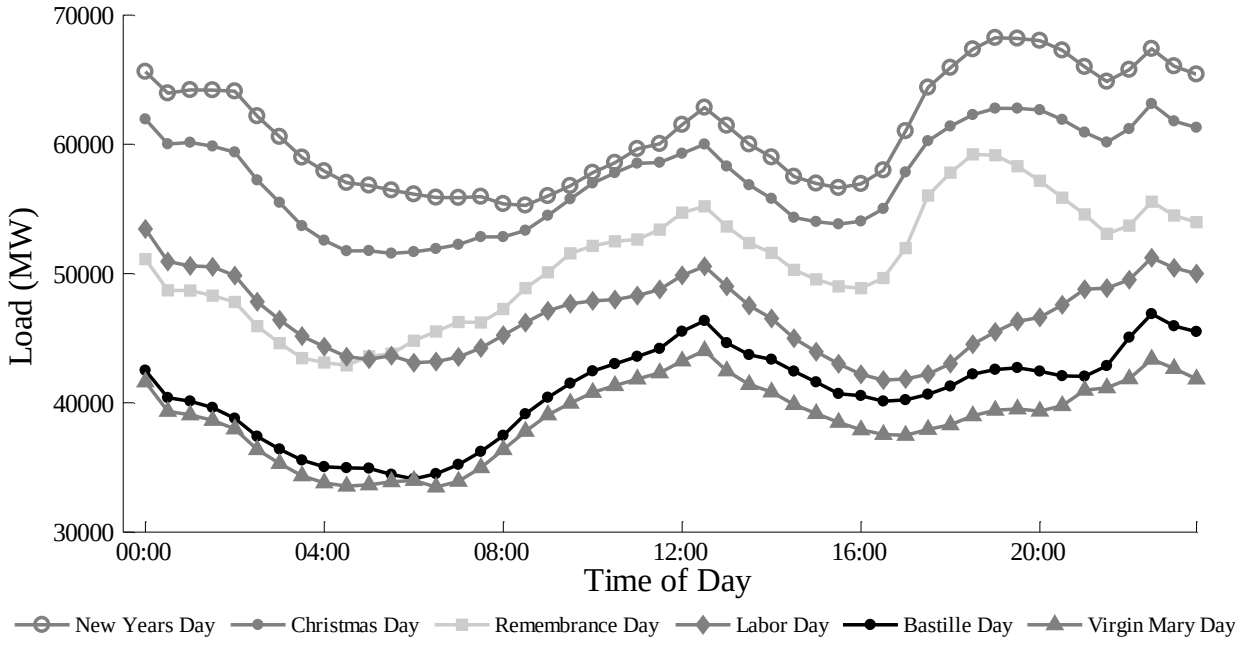

Figure 4— Load profile for a New Year's Day (1 January), Christmas Day (25 December), Remembrance Day (11 November), Labor Day (1 May), Bastille Day (14 July), and The Assumption of Blessed Virgin Mary Day (15 August), observed in the year 2008.

In Figure 4, we plot load profiles for six different special days observed in the year 2008. As expected, load for special days occurring during winter months (New Year's Day, Christmas Day and Remembrance Day) is considerably higher than load for special days occurring during summer months (Labor Day, Bastille Day and The Assumption of Blessed Virgin Mary Day). Moreover, it is interesting to note that the profile for different special days is noticeably different. It is due to this reason, that we do not classify different special days as being the same.

In Figure 5, we plot load for a special day and a corresponding normal day (from the following weeks), for all years within the estimation sample. Specifically, we plot load for a New Year's Day (1 January), and a normal day (14 January), observed across eight years (2001-2008). It can be seen from Figure 5, that the profile for a given special day and the corresponding normal day is different across different years. Both New Year's Day and the normal working day obviously fall on a different day of the week each year. Note that 14 January fell on a Sunday in 2001 and 2007. It is due to this reason that compared to the other years; load on 14 January is relatively low for the years 2001 and 2007 (as shown in Figure 5b). Moreover, we note from Figure 5 that there is no strict trend in load for a given special or a normal day across different years.

We denote the length of the intraday, intraweek, and intrayear seasonal cycle by m_1, m_2 and $m_3(t)$. Since the data is recorded every half-hour, we have m_1 = 48 and m_2 = 336. For normal days, we define $m_3(t) = 52 \times m_2$ (for a given period t), except for few weeks around the clock-change, where we define $m_3(t) = 53 \times m_2$. For special days, we select $m_3(t)$ using a rule-based approach. This allows appropriate selection of historical anomalous load observations in the model, to be extrapolated into future to generate forecasts, as explained further in detail in Section 5.

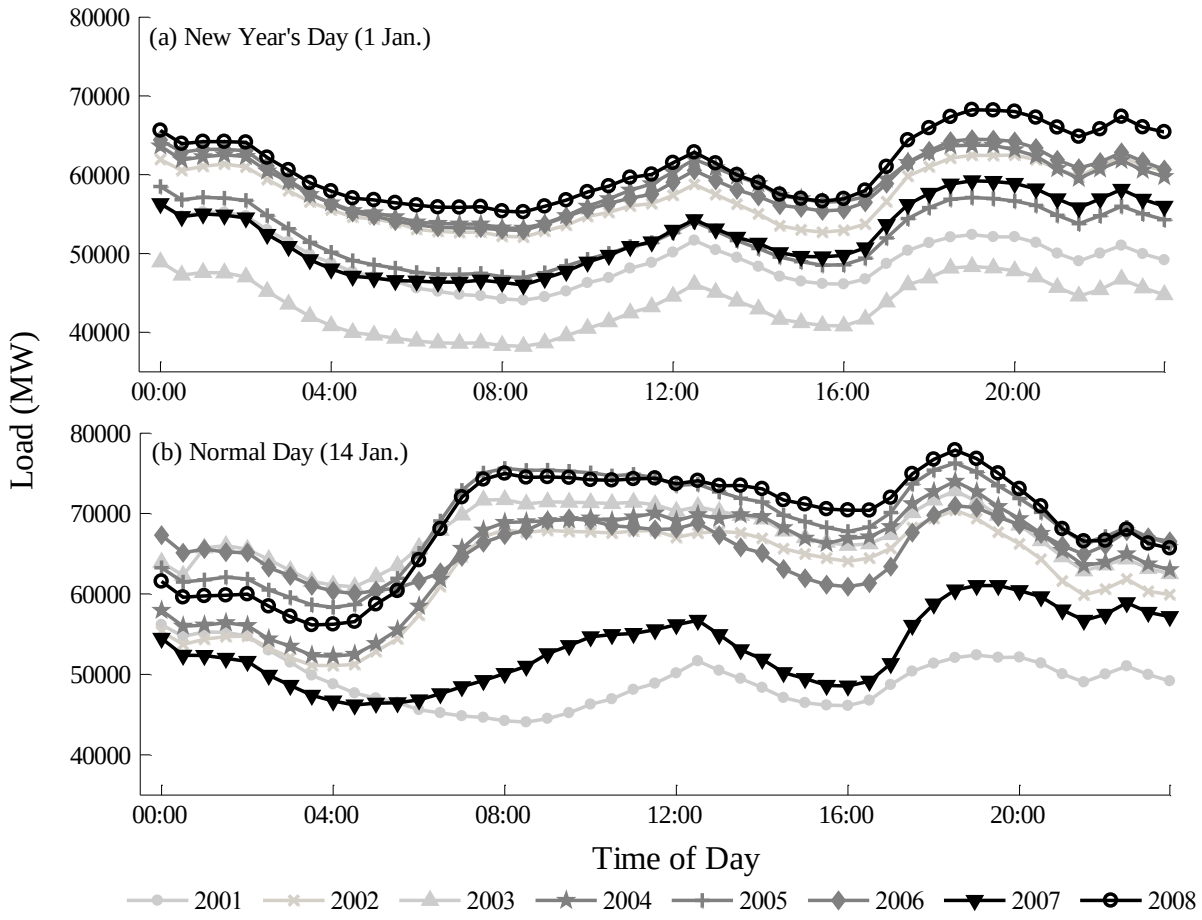

Figure 5— Load profile for a New Year's Day (1 January), and a following normal day (14 January) observed across all years within the estimation sample, stretching from 2001 to 2008.

4. Rule-based Forecasting Methods

4.1. *Rule-based Modified HWT exponential smoothing*

We modify the rule-based HWT exponential smoothing method proposed by Arora and Taylor (2013), to model normal and anomalous load using the following method represented in a single source of error state space form:

$$y_t = l_{t-1} + I_{N_t}\left(d_{t-m_1} + w_{t-m_2}\right) + a_{t-m_{3(t)}} + \phi e_{t-1} + I_{N_t}\varepsilon_t^{(N)} + I_{S_t}\varepsilon_t^{(S)} \quad (1)$$

$$e_t = y_t - \left(l_{t-1} + I_{N_t}\left(d_{t-m_1} + w_{t-m_2}\right) + a_{t-m_{3(t)}}\right) \quad (2)$$

$$l_t = l_{t-1} + \lambda e_t \quad (3)$$

$$d_t = d_{t-m_1} + I_{N_t}\delta e_t \quad (4)$$

$$w_t = w_{t-m_2} + I_{N_t}\omega e_t \quad (5)$$

$$a_t = a_{t-m_3(t)} + I_{N_t}\alpha_1 e_t \; + I_{S_t}\alpha_2 e_t \quad (6)$$

where y_t denotes the load observed at a period t, l denotes the smoothed level, while d, w and a represent the daily, weekly and annual seasonal indices, respectively. The term involving parameter ϕ adjusts for first order autocorrelations in the error, denoted by e_t. The model errors for normal and special days are denoted by $\varepsilon_t^{(N)} \sim NID(0, \sigma_N^2)$ and $\varepsilon_t^{(S)} \sim NID(0, \sigma_S^2)$, respectively, having corresponding variances σ_N^2 and σ_S^2, while NID refers to a normal and independently distributed process. For any period t occurring on normal days, the binary indicator I_{N_t} equals one, and zero otherwise. Similarly, for t falling on special days, I_{S_t} equals one, and zero otherwise. The smoothing parameters are denoted by $\lambda, \delta, \omega, \alpha_1$ and α_2. The length of the intrayear seasonal cycle is denoted by $m_3(t)$, for a given period t. For special days, $m_3(t)$ is selected using a rule based approach, while for normal days, $m_3(t)$ equals either $52 \times m_2$ or $53 \times m_2$ (depending on the clock-change). We refer to this model as rule-based triple seasonal HWT exponential smoothing (RB-HWT).

In the above presented model, the index d accommodates the intraday seasonality for normal days, while w captures the intraweek seasonality for normal days, which remains after the intraday seasonality for normal days has been removed. The index a accommodates intrayear seasonality for normal days, after both the intraday and intraweek seasonality for only the normal days has been deducted. Moreover, for special days, a solely accommodates the intraday, intraweek, and intrayear seasonal effects on anomalous load. Given that special days occur annually, it is convenient to incorporate special day effects via the intrayear seasonal index. Note

that we update a at different rates for normal and special days, using smoothing parameters α_1 and α_2, respectively. This gives the model the flexibility, to be able to allow the impact of normal and special days to be different on the intrayear seasonal index. Furthermore, since d and w accommodate seasonal effects for only the normal days, we do not update these indices on special days.

The HWT exponential smoothing method proposed by Arora and Taylor (2013) focusses on modeling anomalous load in terms of its deviation from normal load, using load for GB. Specifically, to model load for special days, their method employs the daily and weekly seasonal indices for normal days, and adjusts the anomalous load profile accordingly for special days using the annual seasonal index. This relies on the current and historical load profiles to exhibit similar deviation from normal load, for same day of the week, observed around the same date. However, using the French load, we find that this assumption does not hold true. Hence, instead of modeling anomalous load in terms of its deviation from normal load (as done by Arora and Taylor 2013), we model anomalous load as being completely separate from normal load. Specifically, we accommodate the triple seasonality for special days solely via the intrayear seasonal index. We find that this modification in the structure of the model led to a substantial improvement in its forecast accuracy, as presented in Section 6.

The model parameters for RB-HWT are estimated by maximizing log likelihood over the estimation sample. The likelihood function assumes a Gaussian error, for which the variance is different on special days to that of normal days. Specifically, we use the following log likelihood (LL) function:

$$LL = -\frac{n_{ND}}{2}\log(2\pi\sigma_N^2) - \frac{n_{SD}}{2}\log(2\pi\sigma_S^2) - \sum_{t=365\times m_2+1}^{N}\left(\frac{I_{N_t}}{2\sigma_N^2}(\varepsilon_t^{(N)})^2 + \frac{I_{S_t}}{2\sigma_S^2}(\varepsilon_t^{(S)})^2\right) \quad (7)$$

where N is the length of the estimation sample, n_{ND} and n_{SD} are the number of load observations that belong to normal and special days, respectively, excluding the observations from the first year.

4.2. *Rule-based SARMA*

As proposed by Arora and Taylor (2013), we consider the following rule-based adaptation of SARMA to model anomalous load:

$$\begin{aligned} &\Upsilon_p(L)\Phi_{P_1}(L^{m_1})X_{P_2}(L^{m_2})\left(I_{N_t}\Psi\left(L^{m_3(t)}\right) + I_{S_t}\theta\left(L^{m_3(t)}\right)\right)(y_t - c) \\ &= \Omega_q(L)\Theta_{Q_1}(L^{m_1})\Gamma_{Q_2}(L^{m_2})\left(I_{N_t}\Lambda\left(L^{m_3(t)}\right)+I_{S_t}K\left(L^{m_3(t)}\right)\right)\left(I_{N_t}\varepsilon_t^{(N)}+I_{S_t}\varepsilon_t^{(S)}\right) \end{aligned} \quad (8)$$

where y_t denotes load; c is a constant; L denotes a lag operator; $\varepsilon_t^{(N)} \sim NID(0, \sigma_N^2)$ and $\varepsilon_t^{(S)} \sim NID(0, \sigma_S^2)$ are model errors for normal and special days, respectively. Moreover, Υ_p, Φ_{P_1} and X_{P_2} are AR polynomial functions of order p, P_1 and P_2, while Ω_q, Θ_{Q_1} and Γ_{Q_2} are MA polynomial functions of order q, Q_1 and Q_2, respectively. The functions Ψ and Λ accommodate the intrayear seasonal effects for normal days; while θ and K accommodate annual seasonality for special days. The function Ψ is written as:

$$\Psi\left(L^{m_3(t)}\right) = 1 + \eta_1 L^{m_3(t)} + \eta_2 L^{m_3(t)+m_3\left(t-m_3(t)\right)} + \eta_3 L^{m_3(t)+m_3\left(t-m_3(t)\right)+m_3\left(t-m_3\left(t-m_3(t)\right)\right)} \quad (9)$$

where η_1, η_2 and η_3 are constant coefficients. The functions Λ, θ and K can be represented using equation (9), with a difference that each function comprises of a different set of coefficients. We adopted the Box and Jenkins (1970) methodology to select polynomial function orders for AR and MA terms. We consider orders equal to or less than three. We refer to this method as RB-

SARMA. We estimate the model parameters by maximizing the log likelihood function, using a Gaussian error with different variances for normal and special days, as we did for RB-HWT.

4.3. *Rule-based ANN*

ANNs have been widely used for modeling anomalous load (Srinivasan *et al*. 1995; Lamedica *et al*. 1996; Kim *et al*. 2000; Song *et al*. 2000; Arora and Taylor 2013). The advantage of using ANNs for load forecasting is that they are able to model the complex nonlinear relationships between load and weather variables in a nonparametric framework, i.e., without making strong prior assumptions about the true functional form of the data generating process. However, the disadvantage of using ANNs is that there is no well-established systematic approach, or a consensus among researchers, for choosing a suitable ANN architecture, namely, the number of inputs, hidden layers, and units within each hidden layer, for a given dataset.

In this study, we employ a feed-forward ANN method with a single hidden layer and a single output, as employed by Arora and Taylor (2013). We pre-process the data prior to modeling, using a double differencing operator of the form $(1 - L^{m_1})(1 - L^{m_2})$. We difference the output using this operator, and normalize it by subtracting the mean, and dividing by the standard deviation. The input comprises lagged load observations, differenced using the above operator, and normalized to have zero mean and unit standard deviation. As ANNs have been shown to be unsuitable for generating multi-step ahead forecasts (Atiya *et al*. 1999), we build a separate ANN model for each forecast horizon. We select the lags for input variables to be consistent with the SARMA model. Specifically, for the ANN built for horizon h, we use load at the forecast origin, and at the following lags: $1,\ 2,\ m_1 - h,\ 2m_1 - h,\ 3m_1 - h,\ m_2 - h,\ 2m_2 - h,\ 3m_2 - h,$ $LagA = m_3(t) - h, LagB = LagA + m_3(t - LagA - h),$ and $LagC = LagB + m_3(t - LagB - h)$, where $m_3(t)$ denotes the magnitude of the intrayear cycle length defined at the

period t. The value of $m_3(t)$ is selected using a rule-based approach for special days, as done earlier for RB-HWT and RB-SARMA.

We use a sigmoid activation function that nonlinearly maps the inputs to the units in the hidden layer. For mapping the values in the units of the hidden layer to the output, we use a linear activation function. We estimate the link weights by minimizing the one-step ahead sum of squared errors (SSE), and employ regularization parameters, which prevent the network weights from becoming too large (Bishop, 1997). We employ the backpropagation algorithm with learning rate η and momentum parameter μ. The parameter η determines how fast or slow the weights change with respect to the output error. The parameter μ gives more weight to the more recent network weights, and is similar to the smoothing parameter used in the exponential smoothing methods. We estimate the model parameters using cross-validation, employing a hold-out sample corresponding to the last one year of the estimation sample. We refer to this method as RB-ANN.

4.4. *Rule-based Intraweek & Intraday SVD based exponential smoothing*

Statistical methods based on *dimension reduction* have been employed for forecasting a range of intraday time series (see, for example, Shen and Huang 2005, 2008a, 2008b; Taylor 2006; 2010b; 2012). The rationale of employing dimension reduction techniques in conjunction with statistical models is to identify and forecast only those components which capture a major proportion of variance in the time series. This allows for a reduction in the dimensionality of the model to be considered.

In this study, we employ the intraweek singular value decomposition (SVD) based method proposed by Arora and Taylor (2013). As done with RB-HWT, we modify the SVD method of

Arora and Taylor (2013) to model anomalous load as being completely separate from normal load. We refer to this method as the rule-based modified intraweek SVD based exponential smoothing method, denoted as RB-IW-SVD.

Moreover, we propose a rule-based modified intraday SVD based exponential smoothing method, referred to as RB-ID-SVD. The RB-ID-SVD method extends the SVD based method proposed by Taylor (2010b), to model both normal and anomalous load in a unified framework. Based on the similarity in the average intraday cycle for different days of the week (as shown in Figure 2), this method treats a week as consisting of five distinct intraday cycle types. Specifically, the RB-ID-SVD method assumes Tuesday, Wednesday and Thursday to have a common intraday cycle, whereas Monday, Friday, Saturday and Sunday are each assumed to have a distinct intraday cycle. The advantage of RB-ID-SVD is that it uses a single model to update the interday feature series (also referred to as principal components), as opposed to building separate time series models for the feature series, as done by Shen and Huang (2005, 2008a, 2008b), for details, see Taylor (2010b).

As opposed to RB-ID-HWT, which utilizes the similarity between different periods in the intraday cycle, RB-IW-HWT achieves dimension reduction by exploiting the similarity between different periods in the intraweek cycle. A limitation of the RB-ID-SVD method is that it requires the initialization and updating of five different interday feature series for different days of the week. On the contrary, RB-IW-SVD employs a single interweek feature series for all days of the week, resulting in a much simpler model. The model parameters for RB-IW-SVD and RB-ID-SVD were estimated using the maximum likelihood procedure as used for RB-HWT.

5. Rule Formulation

This section formulates a rule based on subjective judgment. The sole purpose of the proposed rule is to determine the value of the intrayear cycle length, $m_3(t)$, in the formulation of the models considered in this study. Using the estimation data, we identified four distinct *features* that have a unique impact on anomalous load. These are the special day type, the period of day, the day of week, and the time of year. For a given special day, the anomalous load profile is treated as a function of the above features.

The rationale of this rule is to treat weekdays as having a different impact on anomalous load, in comparison to weekends, and allow each special day to have a unique profile. This rule is based on the observation that the average intraday load profile for weekends is substantially lower compared to weekdays (as shown in Figure 2), and that different special days exhibit different profiles (as shown in Figure 4).

During the modeling, this rule requires that the current and historical anomalous load observations belong either to a weekday, or a weekend. As an example, consider Boxing Day (26 December) in 2009, which fell on a Saturday. Using this rule, $m_3(t)$ is selected so as to include observations belonging to the most recent occurrence of a Boxing Day, which also fell on a weekend. Hence, this rule refers to Boxing Day in 2004, which was a Sunday. Specifically, for all periods belonging to Boxing Day in 2009, this rule sets $m_3(t) = (4 \times 365 + 366) \times m_2$. Similarly, to model load for New Year's Day (1 January) in 2009, which fell on a Friday, this rule refers to New Year's Day in 2008, which fell on a Thursday, as both special days occur on a weekday. Hence, for all periods belonging to New Year's Day in 2009, we set $m_3(t) = 366 \times m_2$. This rule takes into account the inclusion of additional observations due to leap years.

Several researchers have incorporated proximity day effects while modeling anomalous load (see, for example, Engle 1982; Ramanathan *et al.* 1997, Pardo *et al*. 2002; Dordonnat *et al*. 2008; Kim 2013; Arora and Taylor 2013). The day which either precedes or follows a special day is defined as a proximity day. Due to special day effects, load on proximity days tends to be lower than normal load for same day of the week (around the same date), but higher than corresponding special day. In Figure 6, we plot load for a Christmas Day (25 December), a proximity day (24 December, Wednesday) that precedes the Christmas Day, and a corresponding normal day from the previous week (17 December, Wednesday), all observed in the year 2008. It is evident from the figure that load on the proximity day is noticeably lower than normal load, but considerably higher than anomalous load.

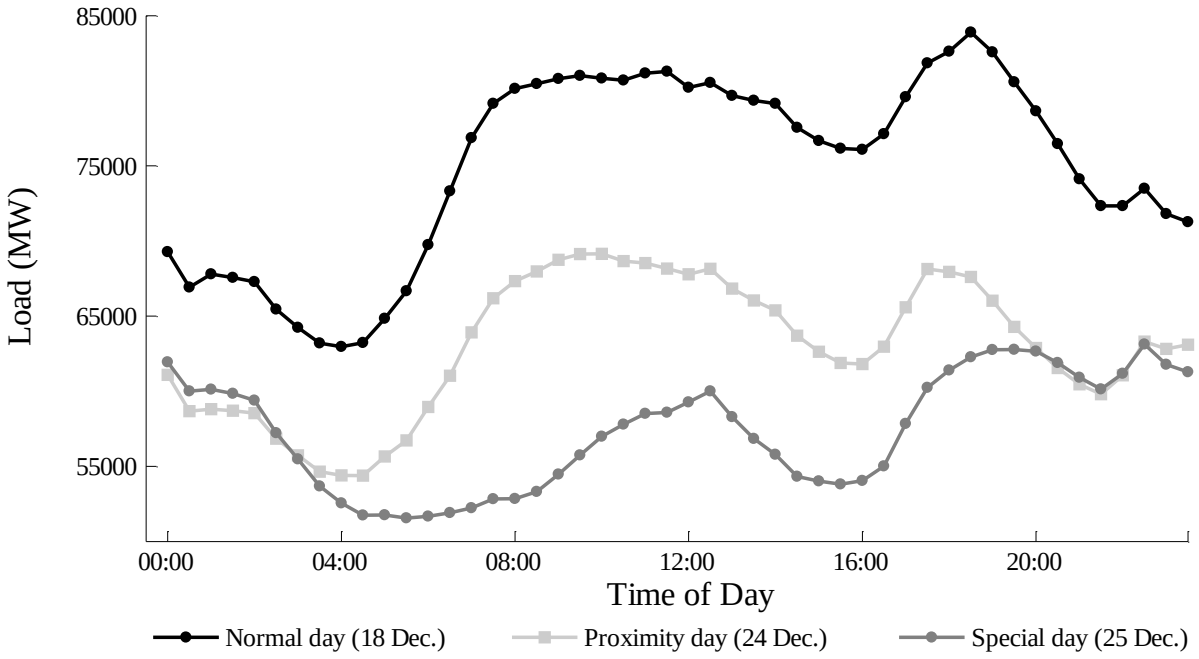

Figure 6— Load profile for a normal day (17 December, Wednesday), proximity day (24 December, Wednesday), and a special day (25 December, Christmas Day, Thursday), all observed in the year 2008.

We denote proximity days using the notation *PD*. For the one year post-sample period (i.e. the year 2009), we identified the following *PDs*: a) 2 January (the day following New Year's

Day), b) 22 May (the day following Ascension Day), and c) 13 July (the day before Bastille Day). Moreover, days within the Christmas period, which either precede a Christmas Day (i.e. 21 December to 24 December, inclusive), or follow a Boxing Day (i.e. 27 December to 30 December, inclusive), are also treated as *PDs*. To appropriately accommodate the impact of special days on *PDs*, we treat *PD*s which follow a special day, as being different from *PD*s which precede a special day. For example, consider 24 December 2009 (Thursday), which is a *PD* preceding a Christmas Day. To model load for this day, we set $m_3(t) = 365 \times m_2$, so that we refer to 24 December 2008 (Wednesday), as both *PD* precede a Christmas Day, and fall on a weekday.

In this study, we also accommodate bridging day effects (see, for example, Dordonnat *et al*. 2008; Arora and Taylor 2013). A bridging day is defined as a proximity day which occurs between a special day and a weekend. Load on *PD* tends to be lowered further if it is a bridging day. Specifically, a Monday preceding a special day, or a Friday following a special day, is defined as a bridging day. Otherwise, it is defined as a non-bridging day. We denote bridging proximity days using the notation *B-PD*, while non-bridging proximity days are referred to as *NB-PD*. We treat *B-PD* as being separate from a *NB-PD*. Moreover, *B-PD* which precede a special day, are treated as being different from *B-PD* which follow a special day. This allows us to appropriately accommodate the impact of special days and weekends on proximity days. For example, consider 2 January in 2009, which occurred on a Friday. We treat this day as a *B-PD*, as it occurs between New Year's Day and weekend. Hence, for all periods on 2 January in 2009, we set $m_3(t) = (3 \times 365 + 2 \times 365) \times m_2$, so that the model refers to observations from 2 January in 2004 (Friday), as both *PD* follow a special day, and belong to the class of *B-PD*. In

cases where the magnitude of $m_3(t)$ tends to be larger than the total number of historical observations using this rule, we simply refer to the same special day from last year.

Using this rule, we identified seven different categories of special day. During the modeling, we ensure that both current and historical special day belongs to the same category. Specifically, for a given special day, we select $m_3(t)$ such that both y_t and $y_{t-m_3(t)}$ adheres to one of the following categories:

Category A: *Basic special days* (national and public holidays) that occur on a weekday.

Category B: Basic special days that occurs on a weekend.

Category C: Bridging proximity days that precede a special day.

Category D: Bridging proximity days that follow a special day.

Category E: Non-bridging proximity days that precede a special day and occur on a weekday.

Category F: Non-bridging proximity days that follow a special day and occur on a weekend.

Category G: Non-bridging proximity days that follow a special day and occur on a weekday.

The category applicable for each special day is specified in Table 1. Note that each special day can be recognized as belonging to one of the seven categories. Specifically, Table 1 presents the complete list of special days observed in the one year post-sample period. For each special day observed in 2009, this table presents the corresponding category, which characterizes the special day under consideration. The table also presents the corresponding historical special day, whose observations are included in the model to generate forecasts. Note that for a given special day, we include observations from only one historical special day during the modeling. These categories can be easily adapted to model anomalous load observations belonging to different datasets. Moreover, this rule is flexible enough to adapt with the inclusion of additional new observations in the model.

TABLE 1: LIST OF SPECIAL DAYS IN FRANCE OBSERVED IN 2009, AND THE CORRESPONDING HISTORICAL SPECIAL DAY REFERRED TO USING THE FORMULALTED RULE.

Current Special Day Type : [*] ***Day of the Week***	**Date (Current Special day)**	**Previous Special Day Referred to via $m_3(t)$**	**Date (Prev. Special day)**
Basic special days that occur on a weekday (**Category A**).			
New Year's Day : *Th.*	01/01/2009	New Year's Day : *Tu.*	01/01/2008
Easter Monday : *M.*	13/04/2009	Easter Monday : *M.*	24/03/2008
Labor Day : *F.*	01/05/2009	Labor Day : *Th.*	01/05/2008
WWII Victory Day : *F.*	08/05/2009	WWII Victory Day : *Th.*	08/05/2008
[**] Ascension Day : *Th.*	21/05/2009	Ascension Day : *Th.*	17/05/2007
Whit Monday : *M.*	01/06/2009	Whit Monday : *M.*	12/05/2008
Bastille Day : *Tu.*	14/07/2009	Bastille Day : *M.*	14/07/2008
Remembrance Day : *W.*	11/11/2009	Remembrance Day : *Tu.*	11/11/2008
Christmas Day : *F.*	25/12/2009	Christmas Day : *Th.*	25/12/2008
New Year's Eve : *Th.*	31/12/2009	New Year's Eve : *W.*	31/12/2008
Basic special days that occur on a weekend (**Category B**).			
Virgin Mary Day : *Sa.*	15/08/2009	Virgin Mary Day : *F.*	15/08/2008
All Saints Day : *Su.*	01/11/2009	All Saints Day : *Sa.*	01/11/2008
Boxing Day : *Sa.*	26/12/2009	Boxing Day : *Su.*	26/12/2004
Bridging proximity days that precede a special day (**Category C**).			
Day before Bastille Day : *M.*	13/07/2009	Day before Bastille Day : *F.*	15/07/2005
Bridging proximity days that follow a special day (**Category D**).			
Day after New Year's : *F.*	02/01/2009	Day after New Year's : *F.*	02/01/2004
Day after Ascension : *F.*	22/05/2009	Day after Ascension : *F.*	18/05/2007
Non-bridging proximity days that precede a special day and occur on a weekday (**Category E**).			
Christmas Week : *M.*	21/12/2009	Christmas Week : *M.*	22/12/2008
Christmas Week : *Tu.*	22/12/2009	Christmas Week : *M.*	22/12/2008
Christmas Week : *W.*	23/12/2009	Christmas Week : *Tu.*	23/12/2008
Christmas Week : *Th.*	24/12/2009	Christmas Week : *W.*	24/12/2008
Non-bridging proximity days that follow a special day and occur on a weekend (**Category F**).			
Christmas Week : *Su.*	27/12/2009	Christmas Week : *Sa.*	30/12/2006
Non-bridging proximity days that follow a special day and occur on a weekday (**Category G**).			
Christmas Week : *M.*	28/12/2009	Christmas Week : *M.*	29/12/2008
Christmas Week : *Tu.*	29/12/2009	Christmas Week : *M.*	29/12/2008
Christmas Week : *W.*	30/12/2009	Christmas Week : *Tu.*	30/12/2008

[*] The seven days of the week are denoted by *M.* (Monday), *Tu. (Tuesday), W.* (Wednesday), *Th.* (Thursday), *F.* (Friday), *Sa.* (Saturday) and *Su.* (Sunday).

[**] Ascension Day in 2008 occurred on the same day as Labor day (1 May 2008), hence, while modeling load for this special day in 2009, we refer to the profile of Ascension Day in 2007 in order to avoid any discrepancy.

6. Empirical Comparison

We provide an empirical comparison of the different methods considered in this study based on an evaluation of their post-sample point and density forecast accuracy. Specifically, we compare the original version and corresponding rule-based adaptations of the different univariate methods presented in Section 4, along with a range of simple benchmarks. To evaluate point forecasts, we use the Mean Absolute Percentage Error (MAPE) and Root Mean Squared Percentage Error (RMPSE) given by:

$$MAPE_h = 100 \times \frac{1}{N-T-h+1} \sum_{i=T+h}^{N} \left| \frac{y_i - \hat{y}_i}{y_i} \right| \tag{10}$$

$$RMPSE_h = 100 \times \sqrt{\frac{1}{N-T-h+1} \sum_{i=T+h}^{N} \left(\frac{y_i - \hat{y}_i}{y_i} \right)^2} \tag{11}$$

where $MAPE_h$ and $RMPSE_h$ denote the MAPE and RMSPE at forecast horizon h, respectively, whereby y_i is the actual load, $\hat{y}_i$ is the corresponding forecast, T is the forecast origin and N is the length of the time series. The relative model rankings were similar for the two measures; hence, we present results using only the MAPE in this paper.

In order to evaluate the density forecast performance, we use the Continuous Ranked Probability Score (CRPS), see Gneiting *et al*. (2007). Note that the CRPS can be viewed as the distributional analogue of the Mean Absolute Error (MAE), and is defined as follows:

$$CRPS = \int_{-\infty}^{\infty} \{F(z) - \mathbf{1}(z \geq y)\}^2 dz \tag{12}$$

where y is the actual observation, and $\mathbf{1}$ denotes an indicator function. The empirical form of CRPS, as given by Gneiting and Raftery (2007), is represented as:

$$CRPS = E_F|Y - y| - \frac{1}{2} E_F|Y - Y'| \quad (13)$$

where Y and Y' are independent samples drawn from the forecasts density function, each having the same distribution F, E_F is the expectation with respect to the distribution F. We use equation (13) to estimate the CRPS as it is relatively convenient to compute compared to equation (12). Note that for $Y = Y'$, i.e. when F reduces to a point forecast, CRPS is same as the MAE.

In this study, we evaluate the original and rule-based adaptations of the HWT exponential smoothing method, SARMA, and the ANN method. Note that the original versions of the univariate methods considered in this study do not incorporate any prior knowledge in the modeling framework using the formulated rule. This amounts to treating special days as normal days during the modeling process. Regarding parameter estimates, for the original HWT exponential smoothing, we estimated λ = 0, δ = 0.3517, ω = 0.0201, α = 0.1048 and ϕ = 0.9940, while for RB-HWT, we estimated λ = 0.0057, δ = 0.0889, ω = 0.0097, α_1 = 0.4661, α_2 = 0.3876 and ϕ = 0.9872. For both original and the rule-based ANN, we obtained η = 0.1, μ = 0.9, number of hidden units m = 30, and regularization parameters to be 0.001. For original SARMA, we estimated the following model:

$$(1 - 0.18L - 0.59L^2 - 0.20L^3)(1 - 0.22L^{m_1} - 0.13L^{2m_1} - 0.23L^{3m_1})(1 - 0.55L^{m_2} + 0.02L^{2m_2})(1 - 0.32L^{Lag1} - 0.22L^{Lag2} - 0.21L^{Lag3})(y_t - 21055) = (1 + 1.02L + 0.57L^2 + 0.20L^3)(1 + 0.03L^{m_1} - 0.03L^{2m_1} - 0.18L^{3m_1})(1 - 0.45L^{m_2} + 0.02L^{3m_2})(1 - 0.13L^{Lag1} - 0.11L^{Lag2} - 0.10L^{Lag3})\varepsilon_t \quad (14)$$

where $Lag1 = m_3(t)$, $Lag2 = Lag1 + m_3\big(t - m_3(t)\big)$, and $Lag3 = Lag2 + m_3\Big(t - m_3\big(t - m_3(t)\big)\Big)$. Moreover, we estimated the following RB-SARMA method:

$$(1 - 0.73L - 0.79L^2 + 0.53L^3)(1 - 0.16L^{m_1} - 0.12L^{2m_1} - 0.12L^{3m_1})(1 - 0.25L^{m_2} - \quad (15)$$

$$0.07L^{2m_2} - 0.09L^{3m_2})\Big(I_{N_t}(1 - 0.23L^{Lag1} - 0.34L^{Lag2} - 0.22L^{Lag3}) + I_{S_t}(1 -$$

$$0.55L^{Lag1} - 0.13L^{Lag2} - 0.12L^{Lag3})\Big)(y_t - 16099) = (1 + 0.39L - 0.28L^2 +$$

$$0.10L^3)(1 + 0.12L^{m_1} - 0.04L^{3m_1})(1 - 0.12L^{m_2} - 0.02L^{2m_2} - 0.04L^{2m_2})\Big(I_{N_t}(1 +$$

$$0.03L^{Lag1} - \ 0.17L^{Lag2} - 0.09L^{Lag3}) + I_{S_t}(1 - 0.16L^{Lag1} + 0.06L^{Lag2} -$$

$$0.11L^{Lag3})\Big)\left(I_{N_t}\varepsilon_t^{(N)} + I_{S_t}\varepsilon_t^{(S)}\right)$$

In Figure 7, we present the MAPE across special days for the original and rule-based adaptations of the HWT exponential smoothing method, SARMA, and the ANN method. It is interesting to see that all the rule-based methods are noticeably more accurate than their corresponding original counterparts, at nearly all horizons. The most accurate method is RB-SARMA, while RB-HWT is the second most accurate method overall. However, the worst performing rule-based method is RB-ANN. The poor performance of RN-ANN can potentially be attributed to the absence of strong nonlinearity in the structure of the time series. Moreover, following Taylor *et al*. (2006), we incorporated an error correction model within the RB-ANN modeling framework. Specifically, if $E_T(h)$ denote the h step ahead forecast error, having corresponding forecast origin denoted by T, the error correction model is represented as $E_T(h) = \phi_h E_{T-h}(h)$. The error correction parameter ϕ_h is estimated separately for each horizon, using ordinary least squares regression, employing only the cross-validation hold out sample (corresponding to last one year of the estimation sample). However, using the error correction term did not lead to a noticeable improvement in the post-sample forecast accuracy of the RB-ANN method. Hence, results for this case are not presented here. Moreover, the RB-ID-SVD and

RB-IW-SVD methods were not competitive with the other univariate methods, and hence, for the sake of conciseness, we do not present results for these methods in this study.

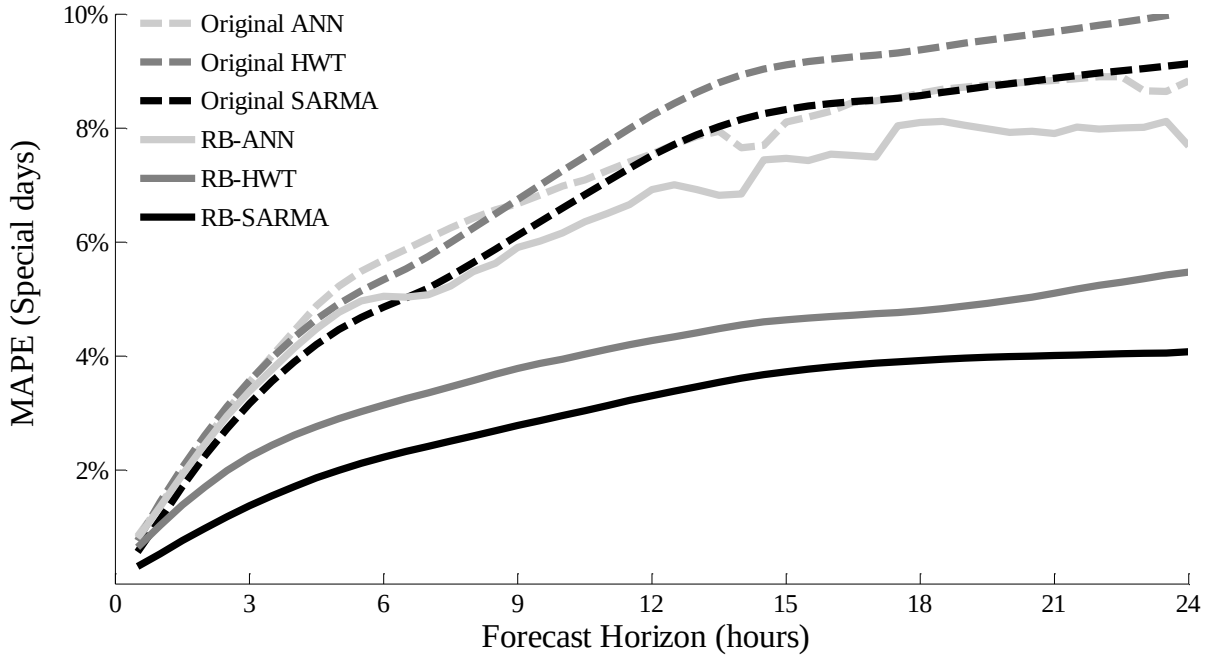

Figure 7— MAPE across special days for the original and rule-adaptations of the HWT exponential smoothing method, SARMA and the ANN method.

In addition to the rule-based methods, we consider the following five simple benchmarks, whereby to model load for a given special day, we use:

1. **Recent Sunday** – load observed on the most recent Sunday. This benchmark was employed by Smith (2000).
2. **Seasonal random walk (SRW)** – load observed on the same special day in the last year.
3. **SRW for same day of the week (SRW-D)** – historical load observed on the same special day, such that both current and previous special day occur on the same day of the week.

4. **Rule-based SRW (RB-SRW)** – historical load observed on the same special day, such that both current and previous special day belong either to a weekday, or a weekend. This benchmark is based on the rule formulated in Section 5.
5. **SRW for same intraday cycle (IC-SRW)** – historical load observed on the same special day, such that both current and previous special day have the same intraday cycle. This benchmark treats a week as consisting of five distinct intraday cycle types, as done for the RB-ID-SVD exponential smoothing method, as discussed in Section 4.4.

For the five simple benchmarks discussed above, the MAPE values across special days are consistently higher than 10% (and lower than 12%), at all horizons considered in this study. The best performing benchmark is RB-SRW, whereas, recent Sunday and SRW are the two worst performing benchmarks. The forecast performance of the original and rule-based adaptations of the univariate methods is significantly superior to the simple benchmarks. The MAPE values for RB-SARMA are about one-third compared to the simple benchmarks. Since the simple benchmarks are not competitive with the rule-based methods, we do not present results for this case in this paper.

In Figure 8, we present the MAPE across special days for the best performing methods from Figure 7 (RB-HWT and RB-SARMA), plotted against different times of the day. Figure 8a presents the MAPE for six-hour ahead forecast, while Figure 8b shows the MAPE for one-day ahead forecast. As expected, the large MAPE values correspond to periods of the day when load changed by a relatively large amount.

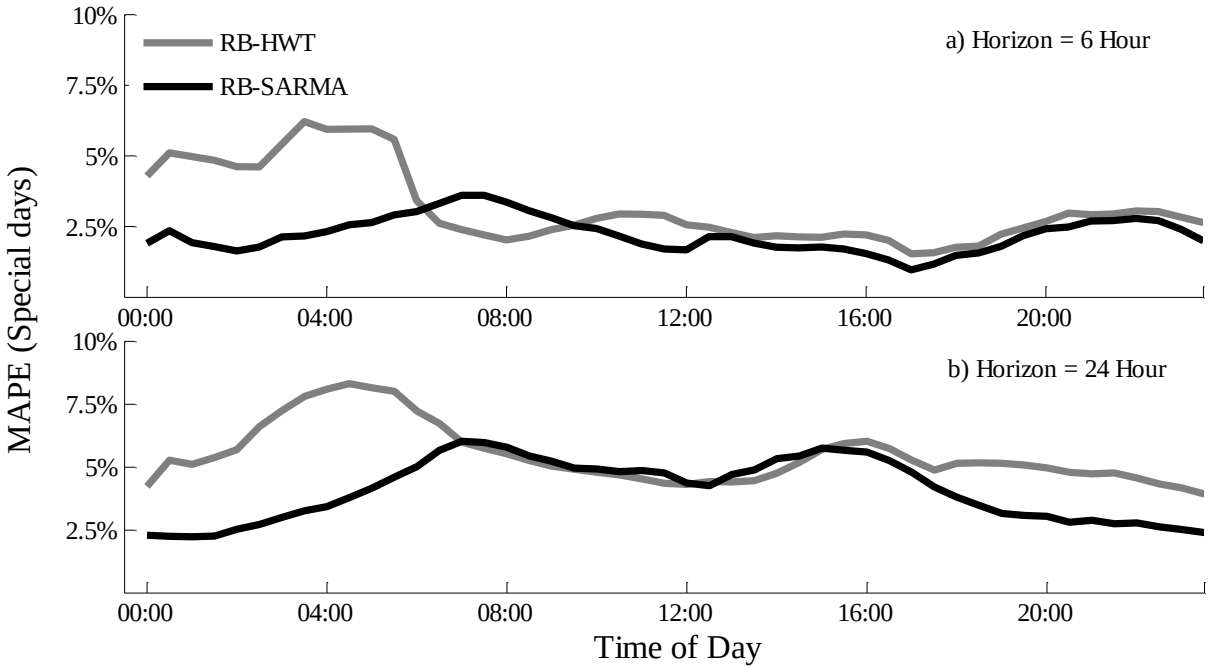

Figure 8— MAPE across special days, using RB-HWT and RB-SARMA, plotted against different time of the day, for forecast horizon equal to: a) six-hour, and b) one-day.

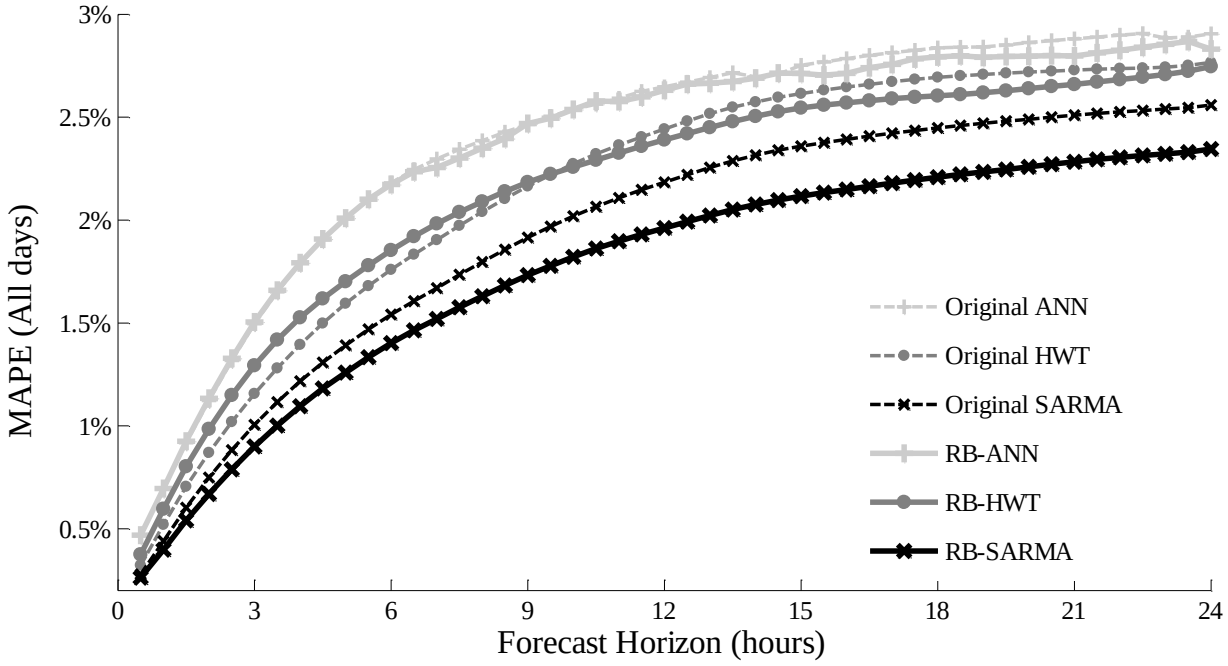

Figure 9— MAPE average across all days for the original and rule-adaptations of the HWT exponential smoothing, SARMA and ANN method.

In Figure 9, we evaluate the methods considered in Figure 8 across all days in the post-sample dataset, i.e. across both normal and special days. It is interesting to see that the overall performance of the rule-based methods is better than their original counterparts. Moreover, RB-SARMA is considerably more accurate than original SARMA at all forecast horizons. It is reassuring to see from this figure that placing emphasis on special days during the modeling results in an improvement in the model's overall performance across all days.

To evaluate density forecast accuracy, in Figure 10, we present the CRPS values across special days for RB-HWT and RB-SARMA. We generated density forecasts using Monte Carlo simulations, whereby for each forecast origin, we used 1000 iterations. It is evident from Figure 10, that RB-SARMA is considerably more accurate than RB-HWT, across both normal and special days. The model rankings based on the CRPS are consistent with the earlier rankings obtained using the MAPE.

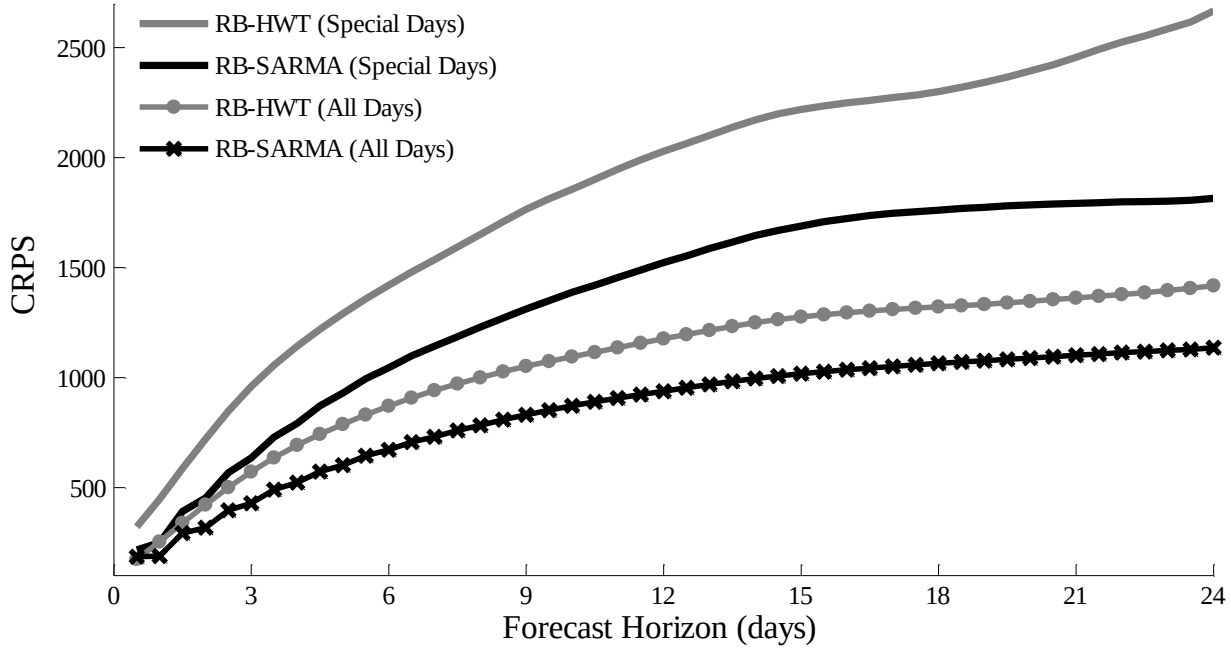

Figure 10— CRPS values for RB-HWT and RB-SARMA averaged across: a) special days, and b) all days. Note that the lower CRPS values are better.

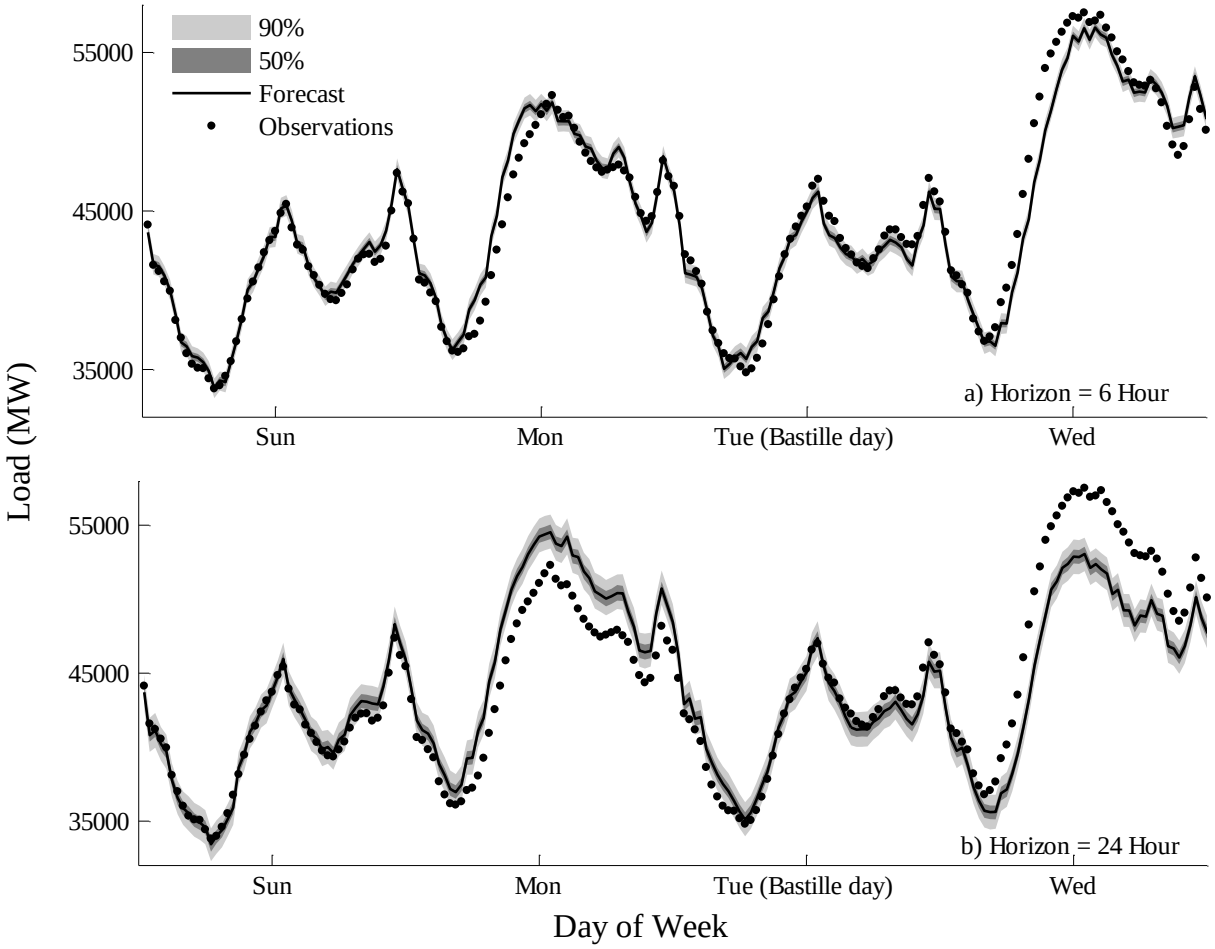

Figure 11— Density forecast generated using RB-SARMA, plotted for forecast horizon corresponding to: a) six-hour, and b) one-day. Note that point forecasts correspond to the median of the predicted density.

In Figure 11, we generate a sequence of six-hour and one-day ahead density forecasts using RB-SARMA, as it is the most accurate model. Specifically, Figure 11 shows density forecasts and corresponding actual observations for four days in the post-sample data, stretching from 12 July (Sunday) to 15 July (Wednesday), inclusive. Note that 14 July (Tuesday) was celebrated as a Bastille Day in France. Hence, we treat 13 July as a bridging proximity day during the modeling, as it was a Monday which preceded a special day. The different shaded regions in Figure 11 correspond to the different quantile ranges (centered around the median) of the

forecast distribution. As expected, the uncertainty associated with the one-day ahead forecast is much higher compared to the six-hour ahead forecasts. Interestingly, RB-SARMA appropriately identifies different day types in the dataset, and adequately models the load profiles for a weekend (12 July, Sunday), bridging proximity day (13 July, Monday), special day (14 July, Bastille Day), and a normal day (15 July, Wednesday), using a unified modeling framework.

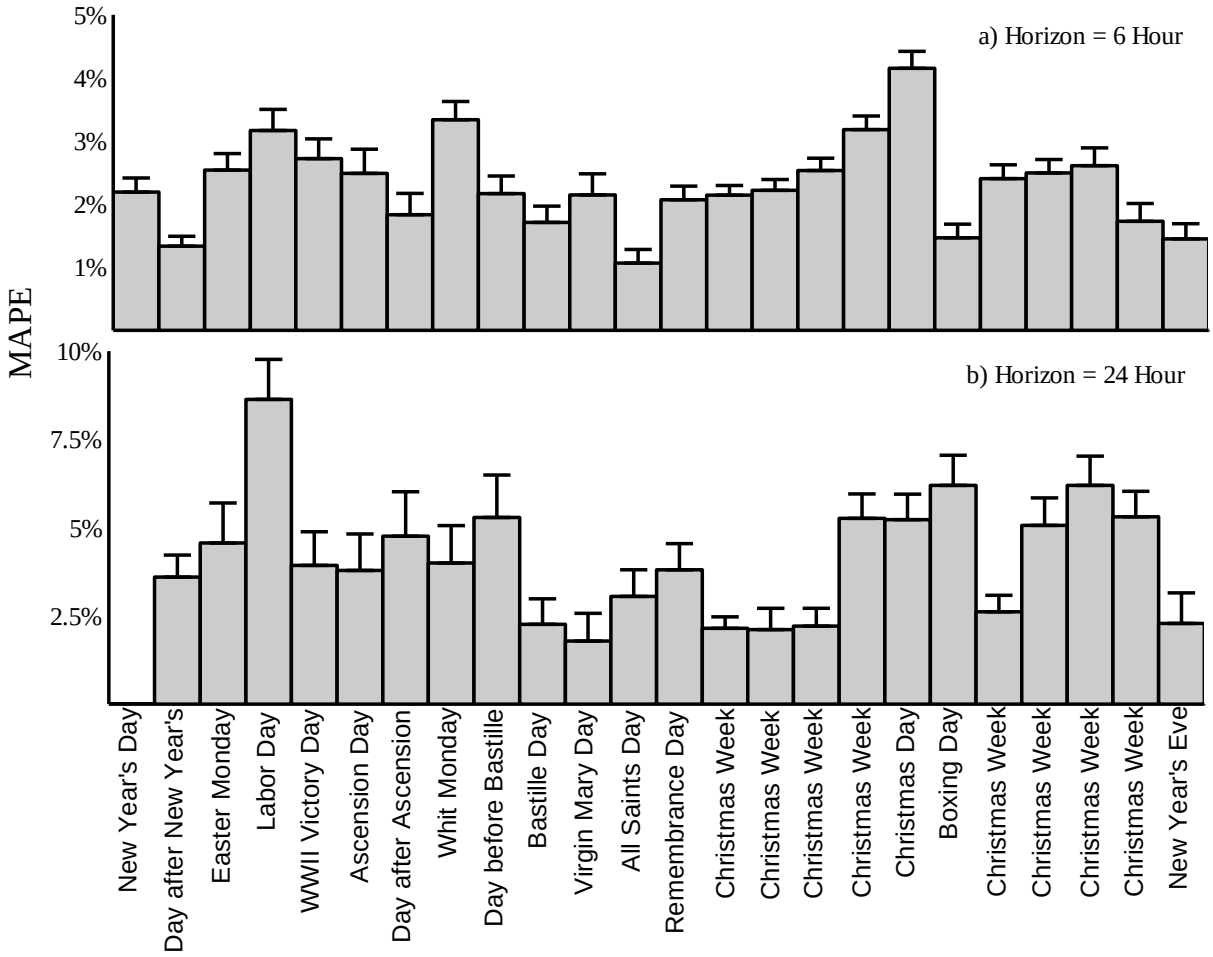

Figure 12— Average MAPE for each individual special day using the RB-SARMA method, and corresponding standard deviation (shown as error bar), plotted for forecast horizon corresponding to: a) six-hour, and b) one-day.

In Figure 12, we plot the MAPE across each individual special day, using RB-SARMA. Note that there are twenty four special days in the one year post-sample data. Specifically, we compute the MAPE associated with each of the 1000 iterations (used in Monte Carlo simulations), for each special day, and report the average MAPE (and corresponding standard deviation). Figure 12a shows MAPEs for six-hour ahead forecast, while Figure 12b presents MAPEs for one-day ahead forecast.

7. Summary and Concluding Remarks

In this paper, we presented a case study on load forecasting for France, with emphasis on special days. We adapted the rule-based methods proposed by Arora and Taylor (2013), and provided an empirical comparison of different methods based on an evaluation of their point and density forecast accuracy. It is noteworthy that previous studies have either ignored special days in the modeling, or focused only on evaluating point forecasts for anomalous load. We investigated the original versions and corresponding rule-based adaptations of five different univariate methods, and five simple benchmarks. Overall, we found that RB-SARMA generated the most accurate forecasts. Interestingly, across special days, the error obtained using RB-SARMA was about one-third compared to the simple benchmarks, and about half compared to the original SARMA method, which was not rule-based. The conclusions of our study are consistent with the recent findings of Kim (2013) and Arora and Taylor (2013), who report that SARMA outperforms methods based on exponential smoothing for anomalous load forecasting.

As opposed to some of the previous approaches, which employ different models for normal and special days, the rule-based methods investigated in this study model load for all days in a unified and coherent framework. This modeling approach makes the task of generating multistep

density forecasts relatively straightforward, which potentially paves the way forward the methods employed in this study to be used to generate real time online forecasts in an automated framework.

An interesting and potentially useful line of future work would be to combine load density forecasts from different models, or adaptively switch between different models based on either the time of day, or the special day under consideration. This would amount to using a different model for different time of the day, or different special days. Moreover, it would be worth investigating the efficacy of the rule-based methods employed in this study, to forecast time series from other applications which exhibit seasonality, and where anomalous conditions pose considerable modeling challenges. Some such examples include time series for call centre arrivals, hospital admissions, cash withdrawals at ATMs, water usage, and transportation counts. For future work, as opposed to using SVD, it would be worth employing the wavelet transform (Daubechies, 1992) and independent component analysis (Comon, 1994) as a tool for dimension reduction for the load data. Furthermore, for horizons longer than a day, and in cases where weather predictions may be easily available, it would be interesting to extend the proposed univariate methods, to also include weather variables as additional explanatory variables, and employ dimension reduction techniques to select only the most relevant variables in the new feature space during the modeling of load data.

Acknowledgement

We would like to extend our sincere gratitude to the International Institute of Forecasters (IIF) and SAS for funding this research. Moreover, we are also very grateful to Pam Stroud for taking care of the administrative issues associated with this grant.

References

Adyaa, M., Collopy, F., Armstrong, J.S. and Kennedy, M. (2000). An application of rule-based forecasting to a situation lacking domain knowledge, *International Journal of Forecasting*, 16, 477–484.

Armstrong, J.S. (2001). Principles of forecasting: A handbook for researchers and practitioners. Kluwer Academic Publishers, Boston.

Armstrong, J.S. (2006). Findings from evidence-based forecasting: Methods for reducing forecast error, *International Journal of Forecasting*, 22, 583–598.

Arora, S. and Taylor, J.W. (2013). Short-term forecasting of anomalous load using rule-based triple seasonal methods, *IEEE Transactions on Power Systems, Forthcoming.*

Atiya, A.F., El-Shoura, S.M., Shaheen, S.I. and El-Sherif, M.S. (1999). A comparison between neural-network forecasting techniques–case study: river flow forecasting, *IEEE Transactions on Neural Networks*, 10, 402–409.

Bishop, C.M. (1997). Neural networks for pattern recognition, Oxford University Press, Oxford.

Bunn, D.W. (2000). Forecasting loads and prices in competitive power markets, *Proceedings of the IEEE*, 88, 163–169.

Bunn, D.W. and Wright, G. (1991). Interaction of judgmental and statistical forecasting methods: issues and analysis, *Management Science*, 37, 501–518.

Cancelo, J.R., Espasa, A. and Grafe, R. (2008). Forecasting the electricity load from one day to one week ahead for the Spanish system operator, *International Journal of Forecasting*, 24, 588–602.

Charytoniuk, W. and Chen, M.-S. (2000). Very short-term load forecasting using artificial neural networks, *IEEE Transactions on Power Systems*, 15, 263–268.

Collopy, F. and Armstrong, J.S. (1992). Rule-based forecasting: development and validation of expert systems approach to combining time series extrapolations, *Management Science*, 38, 1394–1414.

Comon, P. (1994). Independent component analysis: a new concept?, *Signal Processing*, Elsevier, 36, 287–314.

Cottet, R. and Smith., M. (2003). Bayesian modelling and forecasting of intraday electricity load, *Journal of the American Statistical Association*, 98, 839–849.

Daubechies, I. (1992). Ten Lectures on Wavelets, *CBMS-NSF Regional Conference Series in Applied Mathematics*, Society for Industrial and Applied Mathematics.

De Livera, A.M., Hyndman, R.J. and Snyder, R.D. (2011). Forecasting time series with complex seasonal patterns using exponential smoothing, *Journal of the American Statistical Association*, 106, 1513–1527.

Dordonnat, V., Koopman, S.J., Ooms, M., Dessertaine, A. and Collet, J. (2008). An hourly periodic state space model for modelling French national electricity load, *International Journal of Forecasting*, 24, 566–587.

Gneiting, T., Balabdaoui, F. and Raftery, A.E. (2007). Probabilistic forecasts, calibration and sharpness, *Journal of the Royal Statistical Society*, 69, 243–268.

Gneiting, T. and Raftery, A.E. (2007). Strictly proper scoring rules, prediction, and estimation, *Journal of the American Statistical Association*, 102, 359–378.

Hippert, H.S., Bunn, D.W. and Souza, R.C. (2005). Large scale neural networks for electricity load forecasting: Are they overfitted?, *International Journal of Forecasting*, 21, 425–434.

Hyde, O. and Hodnett, P.F. (1993). Rule-based procedures in short-term electricity load forecasting, *IMA Journal of Mathematics Applied in Business and Industry*, 5, 131–141.

Hyde, O. and Hodnett, P.F. (1997). An adaptable automated procedure for short-term electricity load forecasting, *IEEE Transactions on Power Systems*, 12, 84–94.

Kim, K-H., Youn, H-S. and Kang, Y-C. (2000). Short-term load forecasting for special days in anomalous load conditions using neural networks and fuzzy inference method, *IEEE Transactions on Power Systems*, 15, 559–565.

Kim, M.S. (2013). Modeling special-day effects for forecasting intraday electricity demand, *European Journal of Operational Research*, 230, 170–180

Lamedica, R., Prudenzi, A., Sforna, M., Caciotta, M. and Ceccellli, V.O. (1996). A neural network based technique for short-term forecasting of anomalous load periods, *IEEE Transactions on Power Systems*, 11, 1749–1756.

Nowicka-Zagrajek, J., Weron, R. (2002). Modeling electricity demand in California: ARMA models with hyperbolic noise, *Signal Process*, 82, 1903–1915.

Pardo, A., Meneu, V. and Valor, E. (2002). Temperature and seasonality influences on Spanish electricity load, *Energy Economics*, 24, 55–70.

Rahman, S. and Bhatnagar, R. (1988). An expert system based algorithm for short term load forecast, *IEEE Transactions on Power Systems*, 3, 392–399.

Ramanathan, R., Engle, R., Granger, C.W.J., V-Araghi, F. and Brace, C. (1997). Short-run forecasts of electricity load and peaks, *International Journal of Forecasting*, 13, 161–174.

Shen, H. and Huang, J.Z. (2005). Analysis of call center arrival data using singular value decomposition, *Applied Stochastic Models in Business and Industry*, 21, 251–263.

Shen, H. and Huang, J.Z. (2008a). Interday forecasting and intraday updating of call center arrivals, *Manufacturing and Service Operations Management*, 10, 391–410.

Shen, H. and Huang, J.Z. (2008b). Forecasting time series of inhomogeneous Poisson processes with application to call center workforce management, *The Annals of Applied Statistics*, 2, 601–623.

Smith, M. (2000). Modelling and short-term forecasting of New South Wales electricity system load, *Journal of Business, Economics and Statistics*, 18, 465–478.

Soares, L.J. and Medeiros, M.C. (2008). Modelling and forecasting short-term electricity load: A comparison of methods with an application to Brazilian data, *International Journal of Forecasting*, 24, 630–644.

Song, K-B., Baek, Y-S., Hong, D.H. and Jang, G. (2005). Short-term load forecasting for the holidays using fuzzy linear regression method, *IEEE Transactions on Power Systems*, 20, 96–101.

Srinivasan, D., Chang, C.S. and Liew, A.C. (1995). Demand forecasting using fuzzy neural computation, with special emphasis on weekend and public holiday forecasting, *IEEE Transactions on Power Systems*, 10, 1897–1903.

Taylor, J.W., de Menezes, L.M. and McSharry, P.E. (2006). A comparison of univariate methods for forecasting electricity demand up to a day ahead, *International Journal of Forecasting*, 22, 1–16.

Taylor, J.W. (2008). An evaluation of methods for very short-term load forecasting using minute-by-minute British data, *International Journal of Forecasting*, 24, 645–658.

Taylor, J.W. (2010a). Triple seasonal methods for electricity demand forecasting, *European Journal of Operations Research*, 204, 139–152.

Taylor, J.W. (2010b). Exponentially weighted methods for forecasting intraday time series with multiple seasonal cycles, *International Journal of Forecasting*, 26, 627–646.

Taylor, J.W. (2012). Short-term load forecasting with exponentially weighted methods, *IEEE Transactions on Power Systems*, 27, 458–464.